Analysis of Cellular Components by Single-Organelle Resolution

Angelika B. Harbauer,[1,2,3*] Annika Schneider,[4*] and Dirk Wohlleber[4]

[1]Max Planck Institute of Neurobiology, Martinsried, Germany; email: angelika.harbauer@neuro.mpg.de

[2] Technical University of Munich, Germany, TUM School of Medicine , Institute of Neuronal Cell Biology

[3]Munich Cluster for Systems Neurology, Munich, Germany

[4] Technical University of Munich, Germany, TUM School of Medicine, Institute of Molecular Immunology and Experimental Oncology; email: annika.schneider@tum.de, dirk.wohlleber@tum.de

*These authors contributed equally to this article

Keywords

organelles, mitochondria, single-organelle analysis, microscopy, flow cytometry

Abstract

Cellular organelles are highly specialized compartments with distinct functions. With the increasing resolution of detection methods, it is getting clearer that same organelles may have different functions or properties not only within different cell populations of a tissue but also within the same cell. Dysfunction or altered function affects the organelle itself and may also lead to malignancies or undesirable cell death. To understand cellular function or dysfunction, it is therefore necessary to analyze cellular components at the single-organelle level. Here, we review the recent advances in analyzing cellular function at single-organelle resolution using high-parameter flow cytometry or multicolor confocal microscopy. We focus on the analysis of mitochondria, as they are organelles at the crossroads of various cellular signaling pathways and functions. However, most of the applied methods/technologies are transferable to any other organelle, such as the endoplasmic reticulum, lysosomes, or peroxisomes.

1. INTRODUCTION

Eukaryotic cells are highly structured and perform various functions. For increased efficiency, many of their functions have been compartmentalized within smaller cellular subunits, called organelles. Those organelles are specialized with regard to their function, morphology, or chemical properties. Altered function or dysfunction of an organelle, e.g., by intoxication, infection, or genetic disease, may affect not only the organelle but the whole cell/organism.

For functional analysis, organelles are typically purified by cell fractionation and therefore analyzed as pooled samples. Heterogeneity within those organelles isolated from different cells or even from the same cell is therefore poorly understood. This is especially important when isolating organelles from tissues with mixed cell types, such as the brain or liver, or in conditions where only some of the cells exhibit a certain condition, such as during infection or upon malignant transformation. In this review, we describe the current knowledge of state-of-the-art methods that are used to assay properties of individual organelles to identify heterogeneity between different cell types or even within one cell type. We mainly focus on mitochondria, but similar workflows are conceivable for the analysis of other individual membranous organelles such as lysosomes or peroxisomes.

Mitochondria evolved from an endocytic event about 2 billion years ago, when a respiring alpha-proteobacterium was engulfed by the ancestor of eukaryotic cells (1). These endocytosed alpha-proteobacteria allowed the host cells to hijack the respiratory capacity of the bacteria and perform oxidative phosphorylation/respiration, which is still their most important function, and enabled the development of multicellular organisms. However, during evolution mitochondria have become integrative components of cellular metabolism and also serve as important buffers for calcium ions. Finally, mitochondria have been integrated into numerous cellular signaling cascades and developed into the central hub in the regulation of programmed cell death (apoptosis) (2, 3). As nearly all cell types harbor mitochondria, except red blood cells, it is obvious that mitochondrial malfunction affects many different tissues. However, the physiological functions of mitochondria are not similar across the cells and are utilized by different cell types quite differently: The brain is one of the major energy consumers in the body, as it accounts for 20% of the overall oxygen consumption despite comprising only 2% of body weight (4). This consumption is disproportionally distributed between the different cell types found within the brain. Neurons are thought to depend on mitochondria and therefore oxygen for

their efficient ATP production and calcium buffering, whereas astrocytes have a more glycolytic metabolism (5). Even within neurons, differences between axonal and dendritic or synaptic and nonsynaptic mitochondria have been identified, including their protein content as well as metabolic and calcium buffering activities (6–9). Also, other organs display a high dependence on mitochondria: The liver is the key organ for protein, carbohydrate, and lipid metabolism of the body, with hepatocytes as the parenchymal cell type fulfilling all the demands. It is therefore not surprising that hepatocytes contain huge numbers of mitochondria (1,000–2,000 per hepatocyte) to cover the high energy demands and that altered mitochondrial function results in liver disease (10, 11). The central role of mitochondria in hepatocytes is also underpinned by the fact that induction of apoptosis after external death receptor stimulation (e.g., by Fas/CD95) is strictly dependent on mitochondrial cytochrome c release (12).

Because of all these differences between mitochondria from different cell types, or even within the same cell, the necessity to analyze mitochondria at the resolution of a single organelle is compulsory, and the technical requirements for such analysis continue to increase.

2. METHODOLOGY

Most of the methods available for single-organelle analysis are based on fluorescent dyes or proteins that can be targeted to the organelle of interest, which are discussed below.

However, the first high-resolution visualization of mitochondria on a single-organelle level was performed by electron microscopy in 1952 (13). During the following years the technology of electron microscopy progressed and resulted in the development of electron tomography that facilitated the analysis of mitochondria in an three-dimensional (3D) manner and the measurement of mitochondrial function using cytochrome c oxidase labeling (14).

With increasing refinement, light as well as confocal or multiphoton microscopy became the standard method to detect organelles and measure changes in shape, distribution, and function. Undoubtedly, the technique's major strength is its high spatial resolution allowing structures to be detected within an intact cell or tissue slices. This method also makes it possible to discriminate the different properties of organelles/mitochondria from different parts of a cell. For example, mitochondria in cultured T cells (Jurkat cells) become recruited to the immunological synapse and display higher calcium loads (15). Also, mitochondria in neuronal processes differ in their shape and presumably their metabolic capacity, with dendritic mitochondrial displaying

mainly elongated shapes and high membrane potential, whereas axonal mitochondria are small, separate organelles approximately 1 µm in length and with a somewhat lower membrane potential (6). Furthermore, close connection or cross talk, e.g., between the endoplasmic reticulum (ER) and mitochondria, can be analyzed in a temporospatial manner (16). However, microscopic analysis is time consuming, generates large data sets, and is not suitable for high-throughput analysis.

With increasing awareness of the importance of mitochondria for the regulation of several signaling events in cells, researchers aimed to analyze mitochondria also by flow cytometry. Flow cytometry enables high-throughput measurement, which in turn promotes the required statistical analysis and enables the detection of more than 10 different fluorochromes simultaneously. However, in the past, flow cytometers were not sensitive enough to detect very small particles in the size range of mitochondria. The analysis of mitochondria was therefore restricted to bulk detection within a single cell but allowed for detection of mitochondrial mass and functional analysis simultaneously (17). Early analysis of purified mitochondria as single organelles, isolated from the HeLa cell line, showed that those mitochondria were located between 100- to 200-nm polystyrene beads after flow cytometric analysis. Mitochondria are expected to be between 0.5 and 1.5 µm, so the size discrepancy in this study may be due to their small refractive indices (18). We recently measured the size of mitochondria isolated from hepatocytes by flow cytometry using spectral analyzers. Those mitochondria were located between 0.88- and 3-µm polystyrene beads with a mean size of 0.97 µm, which corresponds to the size of the same mitochondria measured by electron microscopy (19) (**Figure 1*a***). The difference between our results and those of the aforementioned study may be because of improved flow cytometers or the origin of the mitochondria (a cell line versus primary hepatocytes). However, caution should be taken when measuring the size of isolated organelles by flow cytometry, as the mitochondrial network may fragment during the isolation process, and the shape of mitochondria may be changed due to the flow in sheath fluidics. The development of highly sensitive flow cytometers and spectral analyzers, which can even detect single virus particles with a diameter down to 27 nm, enabled the analysis of organelles isolated from cells or tissue (20). Single-organelle analysis using flow cytometry has been demonstrated recently for the identification and functional measurement of mitochondria, lysosomes, autophagic vacuoles, and endosomes (19, 21–23). Furthermore, mitochondrial isolation via fluorescent-activated

mitochondrial sorting (FAMS) enables purification of mitochondrial subpopulations according to differential protein expression or membrane potential for further downstream analysis (24). Measuring the proteome of mitochondria from liver tissue or brain tissue purified via FAMS revealed a significant divergence between mitochondrial protein expression between tissues. From 1,858 identified proteins, only 361 were nondifferentially expressed, while 1,492 were highly expressed in liver mitochondria or brain mitochondria (24).

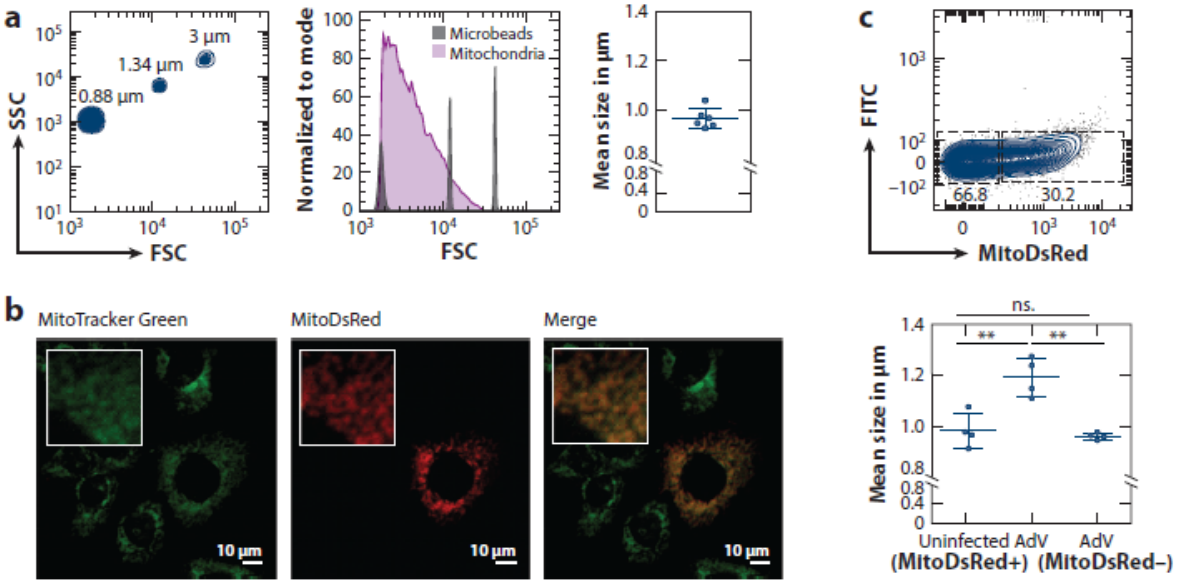

Figure 1 Detection of mitochondria and size measurement. (*a*) Flow cytometric size determination of liver mitochondria using polystyrene particles for calibration. (*b*) Microscopic identification of mitochondria within infected AML-12 cells labeled by a virus-encoded MitoDsRed and counterstained with MitoTracker Green. (*c*) Flow cytometric size determination of mitochondria originating from livers containing virus-infected and noninfected hepatocytes within the same sample. Figure adapted from Reference 19 (CC BY 4.0). Abbreviations: AdV, Adenovirus; FITC, Fluoresceinisothiocyanat; FSC, forward scatter; SSC, side scatter.

Immunoisolation of organelles in a cell type–specific manner has also been successfully applied to mitochondria and lysosomes (25–28). Finally, analysis of mitochondrial DNA (mtDNA) by real-time polymerase chain reaction (PCR) of single mitochondria is becoming more widely used. In this method, single mitochondria are isolated by laser microdissection from individual cells or single mitochondria are picked up with a micropipette guided by prior fluorescence labeling (e.g., MitoTracker Red) (29, 30). Studies showed that mitochondria from a

single cell are heterogeneous with regard to certain (pathogenic) mutations, a phenomenon called heteroplasmy. However, the small sample size and fixatives used in this approach limits the subsequent analysis to highly sensitive transcriptomics, proteomics, or metabolomics. To study organellar function, fluorescent dyes and proteins are the preferred methods, as they can be used in vivo or in cultured living cells.

3. DETECTION OF DIFFERENT CELLULAR ORGANELLES

Over time, many probes have been developed that can easily be used to stain and identify the organelle of interest, such as LysoTracker for lysosomes or MitoTracker for mitochondria. These probes take advantage of the specific environments or characteristics of the organelle, such as the low pH within lysosomes or free thiol groups of specific cysteine residues present in mitochondrial proteins, which are probed by MitoTracker Green (31). Other organelles such as peroxisomes or endosomes are less accessible for this type of small-molecular dye. Therefore, genetically encoded fluorescent markers have been developed for virtually all known organelles to allow visualization and tracking of organelle size, shape, and dynamics. To achieve this, a resident protein or targeting signal is fused to a fluorescent reporter protein and expressed by transfection or transduction in the cell type or tissue or interest. **Table 1** lists common targeting sequences used to target reporter proteins to the respective localization.

Table 1 Common fusion sequences to target distinct organelles

Organelle of interest	Fusion protein/targeting signal	Localization within organelle
Mitochondria	Cox8a N-terminal targeting sequence Su9 N-terminal targeting sequence	Matrix
Mitochondria	OMP25 transmembrane domain (C-terminal) Fis1 transmembrane domain (N-terminal) AKAP1 transmembrane domain (N-terminal) CISD1 transmembrane domain (N-terminal)	Outer membrane–facing cytosol
Lysosomes	Lamp1 rMCP	Membrane-associated, facing cytosol Within secretory lysosome
Lysosomes	TMEM192	Membrane-associated, facing cytosol
Peroxisomes	Amino acid sequence SKL at C terminus	Lumen
Peroxisomes	Pxmp2	Membrane-associated, facing cytosol
Early endosomes	Rab5	Membrane-associated, facing cytosol
Late endosomes	Rab7a	Membrane-associated, facing cytosol
Endoplasmic reticulum	Amino acid sequence KDEL at C terminus	Lumen
Endoplasmic reticulum	Cb5 transmembrane domain (C-terminal)	Membrane-associated, facing cytosol
Golgi	B4GALT1	Golgi membrane stacks, facing lumen
Golgi	TGOLN2	Trans Golgi network, facing lumen
Nucleus	Nuclear import sequence (e.g., from SV40)	Nuclear lumen

Microscopic inspection of these constructs yields information on organellar abundance, size, and shape. For example, a fusion protein of a mitochondrial targeting sequence and DsRed, which was encoded by an adenoviral construct, has been used to label mitochondria from virus-infected cells (**Figure 1*b***). Size determination of mitochondria from those adenovirus-infected hepatocytes showed an enlargement compared to mitochondria from uninfected hepatocytes (**Figure 1*c***).

In addition, time-lapse imaging can be used to observe dynamic changes in individual organelles, such as small range movements or transport along microtubules. Many organelles are highly dynamic, such as the ER and mitochondria, which undergo frequent remodeling of their networks. Such changes can be indicative of functional alterations. For mitochondria, fragmentation of the mitochondrial network is often indicative of mitochondrial stress and may even precede the induction of apoptosis (3, 32). However, the extent of mitochondrial fragmentation under basal conditions is highly variable and dependent on the metabolic state of the cell (33). Furthermore, mitochondrial division can even prevent spreading of a calcium wave preceding apoptosis (34). Therefore, mitochondrial shape is only a limited proxy for cellular and mitochondrial health, and any changes detected should be followed up by functional assays interrogating the membrane potential, mitochondrial calcium content, or the induction of apoptosis.

4. DETECTION AND MEASUREMENT OF MITOCHONDRIAL FUNCTION

Mitochondria are highly complex organelles, originally capable of performing oxidative phosphorylation. However, during their evolution, mitochondria acquired many more roles in regulating cell-intrinsic signaling, metabolism, and storage, which are discussed below.

4.1. Membrane Potential and pH

A key feature of the respiratory chain/oxidative phosphorylation is the transport of protons across the inner mitochondrial membrane, resulting in a negative charge within the mitochondria. Therefore, many cationic fluorescent dyes accumulate in the mitochondrial matrix in dependence of the mitochondrial membrane potential. This can be used as a readout to measure the mitochondrial membrane potential, as a higher staining intensity will correlate with the higher activity of the respiratory chain. How this then relates to the production of ATP is not as

straightforward (35), and even within mitochondrial subcompartments, the differences can be detected (36). Nevertheless, this method can be used as a reliable measure to judge mitochondrial health and the activity of the respiratory chain. Well-known examples include the fluorescent cationic dyes rhodamine-123 and $DiOC_6$ (3,3′-dihexyloxacarbocyanine iodide), $DilC_1(5)$ (1,1′,3,3,3′,3′-hexamethylindodicarbocyanine iodide), TMRE (tetramethylrhodamine, ethyl ester), TMRM (tetramethylrhodamine, methyl ester), and JC-1 (5,5,6,6′-tetrachloro-1,1′,3,3′ tetraethylbenzimidazoylcarbocyanine iodide). Upon mitochondrial depolarization, the staining intensity for most of these dyes will be reduced and eventually be lost. The dye intensity can be read out using microscopy (TMRE; **Figure 2*a***), or flow cytometry of individual organelles [$DilC_1(5)$; **Figure 2*b***]. As an exception, the green fluorescent cationic dye JC-1 forms a concentration-dependent complex upon membrane potential–dependent import into mitochondria. This reversible complex exhibits red-shifted fluorescence (37). Hence, healthy mitochondria will exhibit a higher red to green ratio due to the higher concentration of JC-1 within the matrix. However, the red JC-1 complexes have been reported to be sensitive to H_2O_2, and differences in local availability of the JC-1 monomer can skew the analysis (reviewed in 38); therefore, TMRE or TMRM may yield more reliable measurements. For an in-depth description on the use of dyes to study the mitochondrial membrane potential, see Reference 38.

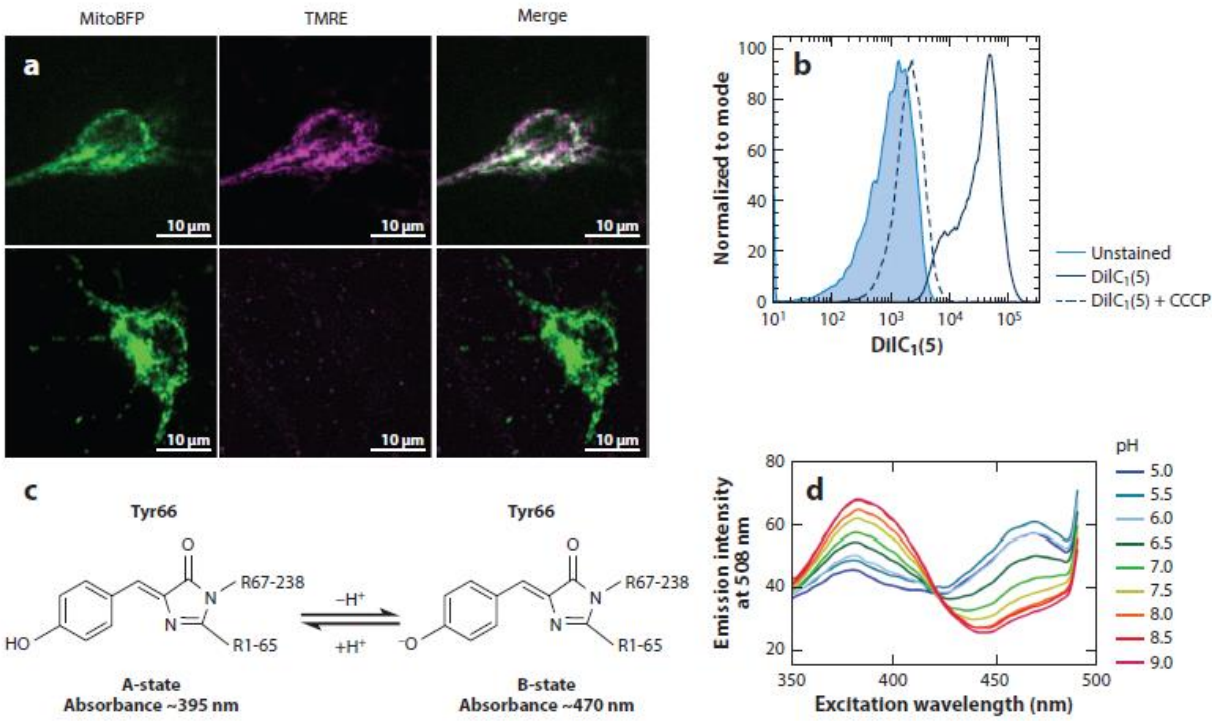

Figure 2 Detection of mitochondria and measurement of membrane potential. (*a*) Microscopic identification of mitochondria in cultured neuronal cell bodies by MitoBFP expression and detection of membrane potential by TMRE. Membrane potential was disrupted by addition of 20 µM antimycin A (*lower row*) (*b*) Measurement of mitochondrial membrane potential of isolated liver mitochondria by DilC1(5) using flow cytometric analysis. Membrane potential was disrupted using 5 µM CCCP. Panel *b* reproduced from Reference 19 (CC BY 4.0). (*c*) Schematic drawing of protonated and deprotonated tyrosin 66 (Tyr66) residue of GFP. (*d*) Schematic drawing of emission intensity at 508 nm of a superfolder GFP in dependence of the pH. Panel (D) reproduced from Reference 44 (CC BY 4.0). Abbreviations: CCCP, Carbonylcyanide-*m*-chlorophenylhydrazone; GFP, green fluorescent protein; TMRE, tetramethylrhodamine, ethyl ester.

As the mitochondrial membrane potential is generated by the extrusion of protons across the inner membrane, dyes or sensors that measure the pH of the matrix (pH_m) can also give an indication about mitochondrial function. Although pH_m was traditionally determined in isolated mitochondria, dyes such as the ratiometric probe SNARF-1 (39) or pH-sensitive green fluorescent protein (GFP) variants are now available (**Figure 2*c*** shows a schematic of pH changes to GFP structure) (40). A commonly used GFP variant, termed pHluorin, was initially used to measure large changes in pH, such as upon externalization of synaptic vesicles [pH values of approximately 5.2 inside the vesicles to neutral pH in the extracellular space (41)]. Mechanistically, protonation of the central fluorophore in pHluorin leads to loss of fluorescence

at low pH, becoming virtually nonfluorescent at a pH lower than 6 at 475 nm excitation. Excitation at 395 nm can still weakly excite pHluorin, and further pHluorin derivates as ratiometric probes have been developed that allow precise measuring of the pH by comparing the fluorescent intensities at 395 nm versus 475 nm excitation (**Figure 2*d***). This approach has been successfully used to measure the pH inside yeast mitochondria or mammalian peroxisomes (42, 43). Recently, a superfolder version was developed that has improved folding capacity and thereby also enables visualization within the ER (44). However, the pK_a of pHluorin variants is between 6.9 and 7.1 (40), which is not ideally suited to measure pH changes in the mammalian mitochondrial matrix with a pH around 7.5 to 8. For this purpose, a derivative of circularly permutated yellow fluorescent protein has been used ($pK_a = 8.7$) (45). This method yielded insights into the coupling of mitochondrial pH and membrane potential as well as evidence for rapid equilibration between adjacent mitochondria without complete matrix exchange (45). This intraorganellar communication within one cell is becoming increasingly more evident (reviewed in 46) and can only be assayed by methods that enable the identification of individual mitochondria in situ.

4.2. Degradation and Turnover

A special case of acidification occurs upon uptake of an organelle into an autophagosome and its subsequent fusion with acidic lysosomes. Two approaches have been described: the use of the acid-stable fluorescent protein Keima (47), which represents a ratiometric fluorescent protein with two excitation maxima modulated by pH, or the combination of acid-labile GFP in tandem with stable mCherry (48) (**Figure 3*a*** shows a schematic of autophagy with Keima, and **Figure 3*b*** illustrates an example image from a neuron). In the latter case, healthy organelles will be double-labeled by GFP and red fluorescent protein, whereas upon autophagy the green signal will be quenched, leading to exclusive red labeling. This approach has been used to assay general autophagy [cytosolic Keima (48) or GFP-mCherry fused to the autophagosomal protein LC3B (49)] as well as specialized receptor-mediated autophagy of individual organelles or protein complexes, including mitochondria and ribosomes (50; also reviewed in 51).

For both sensors, mouse lines have been generated that target the autophagy reporter to mitochondria in order to assay mitophagy in vivo (52, 53). This has led to the puzzling observation that basal mitophagy in neurons remains unchanged upon loss of the mitophagy sensor PTEN-induced kinase 1 (PINK1) (54). PINK1 has an established role in the detection of

mitochondrial dysfunction, as its mitochondrial import is redirected from the inner to the outer mitochondrial membrane upon loss of the mitochondrial membrane potential, which initiates a cascade that marks the organelle for mitophagy (reviewed in 55). As loss-of-function mutations in PINK1 lead to Parkinson's disease, it had been assumed that this pathway would be extremely important in neurons (56). However, this view is challenged by the abovementioned findings. Interestingly, PINK1 knockout mouse models also do not develop Parkinsonian phenotypes, unless they are hit by a second mutation or stressed by mitochondrial toxins (reviewed in 57). In line with this, upon prolonged aging in a *Drosophila* model, there is a loss of mitophagy in PINK1-null mutants observed when using a mitophagy sensor in fly neurons (58). Alternatively, other mitophagy pathways may be upregulated to compensate for the loss of PINK1.

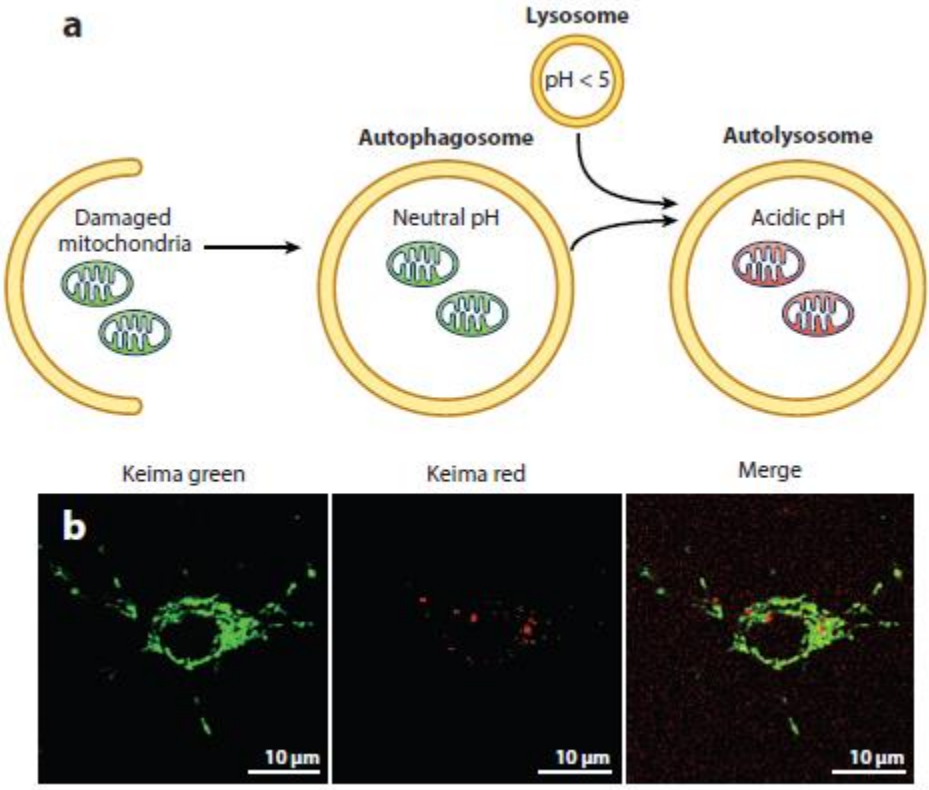

Figure 3 Identification of basal mitophagy by mito-Keima. (*a*) Schematic drawing illustrating the pH-dependent shift in Keima-labeled mitochondria upon fusion of the autophagosome with the acidic lysosome. Green = neutral pH: mitochondria localized within cytosol or neutral Autophagosome, red = low pH: mitochondria localized within acidic Autolysosomes. (*b*) Microscopic identification of cytosolic mitochondria (*green*) and mitochondria in autolysosomal vesicles (*red*) by mito-Keima within cultured neuronal cell bodies.

Mitochondrial turnover does not only include mitophagy, but several pathways can degrade mitochondrial contents, including mitochondrial proteases or mitochondrially derived vesicles (59, 60). It is therefore difficult to estimate the overall lifetime of this organelle. Attempts have been made to study mitochondrial lifetime using fluorescent timer proteins such as MitoTimer (61) or monitoring mitochondrial fate after photoconversion of a photoswitchable fluorophore (62). However, as these sensors are expressed as soluble matrix proteins, their turnover only reflects a part of the mitochondrial protein content. Recently it was shown that some mitochondrial proteins, especially components of the inner membrane respiratory complexes, are stable for several months and avoid turnover by mitophagy or mitochondrial proteases (63). This is one limitation of sensor-based single-organelle analysis, which can be overcome by the use of high-throughput methods such as mass spectrometry of individual organelles.

4.3. Calcium Storage

Rapid intracellular calcium dynamics depend on the clearance of free calcium from the cytosol to shut off ongoing calcium mediated signaling (64). Many calcium binding proteins in the cytosol, such as parvalbumin, can serve as calcium buffers, but most effectively calcium is removed by export across the plasma membrane or by storing of calcium in intracellular calcium stores like the ER or mitochondria (64). Calcium uptake also actively regulates mitochondrial metabolism through stimulation of several dehydrogenases within the tricarboxylic acid (TCA) cycle (65). However, high mitochondrial calcium load or impaired calcium-buffering capacity has been linked to the opening of the mitochondrial permeability transition pore and induction of apoptotic or necrotic processes (66, 67). Measuring mitochondrial calcium content therefore has important implications for cellular health. Although small-molecule dyes such as rhod-2/AM (AM, acetoxymethyl ester) are available (68), genetically encoded calcium sensors have taken center stage owing to their improved targeting to mitochondria and their ability to be expressed exclusively in the cell type of interest (69). Most sensors make use of the tight interaction between calmodulin and the M13 peptide from the myosin light chain kinase upon calcium binding, which is read out as either the Förster resonance energy transfer (FRET) distance between two fluorophores or as a change in intensity of circularly permutated GFP versions (70) (**Figure 4**).

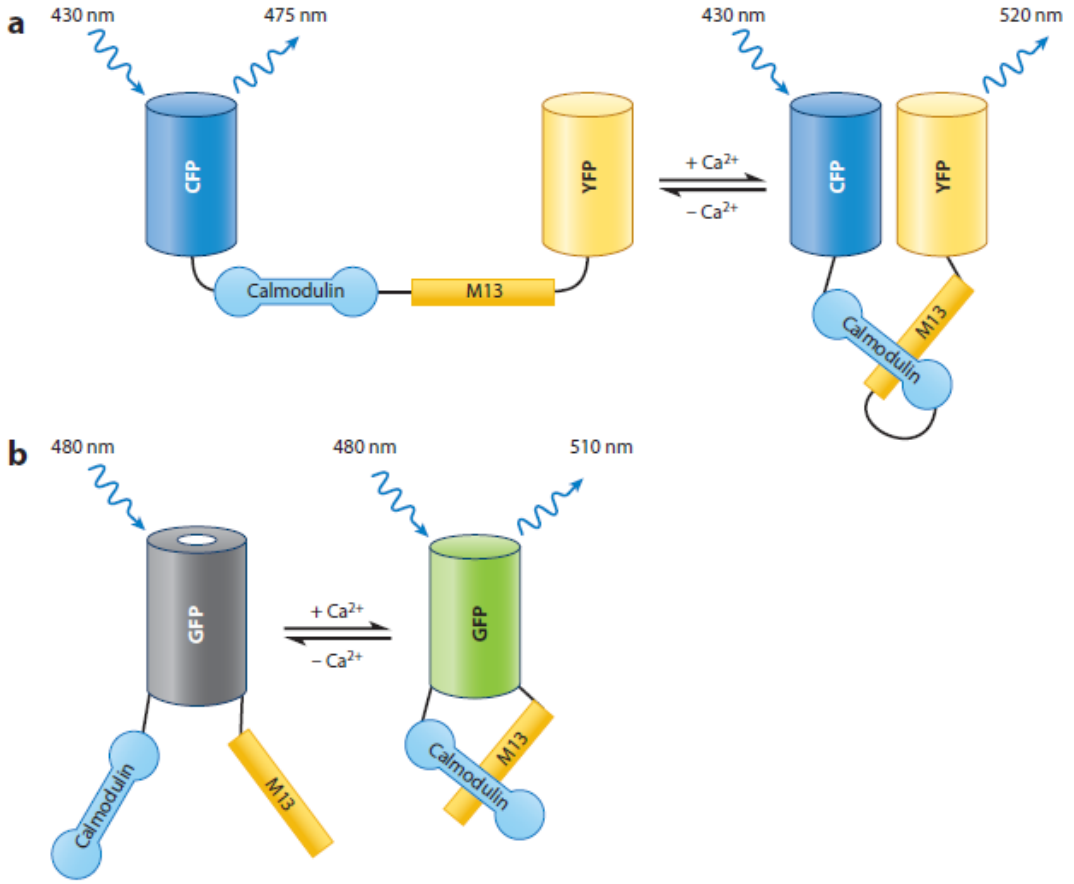

Figure 4 Working principle of genetically encoded calcium sensors. (*a*) A FRET-based construct allows the transfer of energy between donor and acceptor fluorophores only in the presence of Ca^{2+} ions due to a conformational change that brings the two fluorophores closer together. (*b*) GCaMP is based on a circular permutation of GFP that is only weakly fluorescent unless interaction of the calmodulin and M13 peptide domains in the presence of Ca^{2+} ions reconnects the N and C terminus and allows proper folding of GFP. Abbreviations: CFP, cyan fluorescent protein; FRET, Förster resonance energy transfer; GCaMP, fusion protein of GFP, calmodulin (CaM) and M13 Peptide; GFP, green fluorescent protein; YFP, yellow fluorescent protein.

Using such sensors, researchers have successfully measured calcium fluctuations in the ER, mitochondria, Golgi, secretory vesicles, cell nucleus, and peroxisomes, but also in subcellular structures such as the plasma membrane or cilia (reviewed in 70). When used in neurons, mitochondrially targeted calcium sensors revealed that mitochondrial calcium uptake via the mitochondrial calcium uniporter (MCU) increases synaptic excitability (71). As not all presynapses contain mitochondria, this implies that mitochondria-free synapses would have higher cytosolic calcium levels and delayed clearance. Indeed, it was shown that the presence of a mitochondrion lowered the presynaptic mean calcium load and delayed synaptic vesicle release

upon repeated stimulation in an MCU-dependent manner (72). Expression of MCU subunits is, however, heterogeneous between neuronal cell types, as identified by single-organelle analysis using immunocapture (25). Interestingly, this study found that the low expression of MCU in cerebellar Purkinje cells was counterbalanced by high expression of Rmdn3, a component of an ER-mitochondria contact site involved in calcium transfer independent of the MCU (73). Only studies such as these focused on single-organelle analysis can reveal cell type–specific differences in mitochondrial calcium handling. As mitochondrial responses to calcium influx within one cell can also be vastly different (74), we predict that within individual cells the ways that mitochondria take up calcium may also be influenced by their protein content and surrounding organelles.

4.4. Apoptosis and Mitochondrial Outer Membrane Permeabilization

Apoptosis is a highly and complex regulated pathway that is critical for regulation of development (75) and differentiation (76), to maintain tissue homeostasis, and for the elimination of malignant transformed (77) or (virus-) infected cells (78). Deregulation of this pathway is thought to be central for various diseases, including cancer.

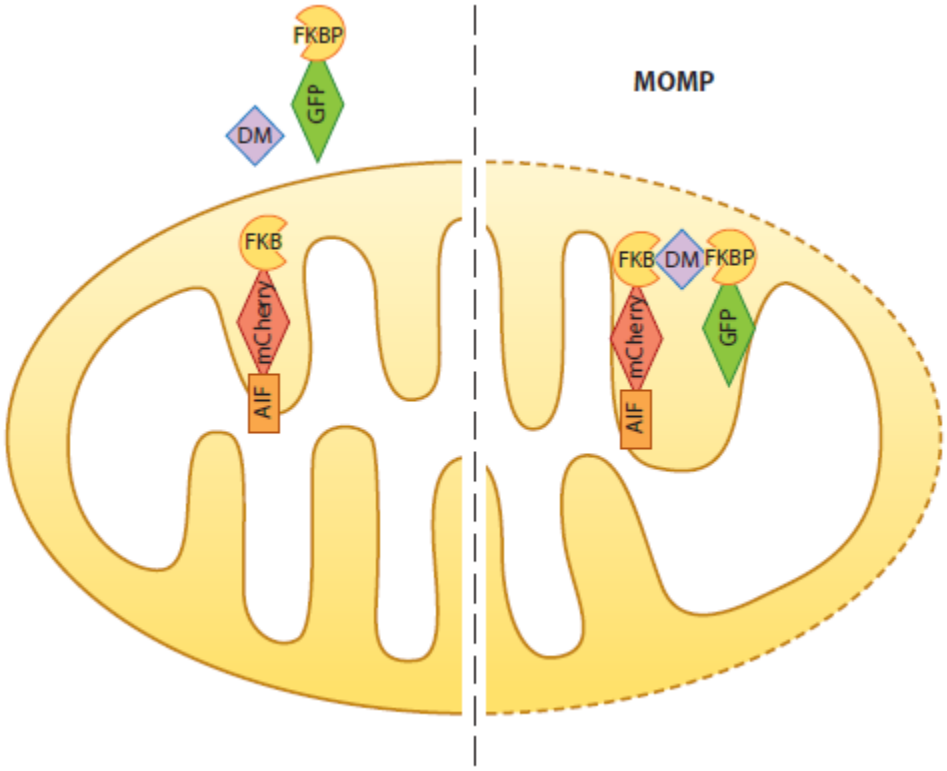

Figure 5 Identification of mitochondrial outer membrane permeabilization (MOMP). In intact mitochondria, the outer membrane separates the green and red fluorophores coupled to the dimerizing proteins FRB and FKBP even in the presence of the dimerizer (DM). In the case of MOMP, both the DM and the GFP-tagged FKBP become accessible to the inner mitochondrial membrane (IMM)-localized FKB-mCherry, which will recruit the cytosolic green fluorescence to mitochondria. Figure adapted from Reference 92 (CC BY 4.0

Depending on the apoptosis-initiation signal, the extrinsic (death receptor–mediated) and intrinsic (mitochondrial) apoptotic pathways are distinguished (79). Whereas the extrinsic apoptotic pathway is initiated upon death receptor signaling at the cell membrane, the intrinsic apoptotic pathway is induced by diverse intracellular stress signals. The (DEFINE) BCL-2 (B-cell lymphoma 2) effector proteins BAX and BAK, which are activated upon the integration of several intracellular stress signals (80, 81), induce disruptions in the outer mitochondrial membrane. These lead to the subsequent release of intermembrane space proteins, most importantly cytochrome c, which drives robust downstream caspase activation (82), a process termed mitochondrial outer membrane permeabilization (MOMP). However, the different pathways may be interconnected because some cell types, such as hepatocytes, depend on the truncated BCL-2 family protein Bid (tBid) and MOMP, despite triggering of the extrinsic pathway (83). MOMP was considered the so-called point of no return, as cells with ruptured mitochondrial membranes typically also die even in the absence of caspase activation, which occurs due to either progressing mitochondrial dysfunction (84, 85) or caspase-independent killing via proteins released from mitochondria (86). Live-cell imaging using GFP-tagged cytochrome c suggested that MOMP occurs synchronously and completely throughout a cell (87). However, it was demonstrated that some cells can survive MOMP (88–90).

Technological progress in single-cell live cell imaging approaches revealed that MOMP does not always occur completely throughout a cell, but that there are differences between individual mitochondria within one cell. In a cell that survives MOMP, a minority of mitochondria evade permeabilization, and those few intact mitochondria can repopulate the surviving cell (91). Using a new approach that enables detection of MOMP in individual mitochondria by the relocalization of fluorescent reporters through chemically dimerizable FKBP/FRB domains, researchers demonstrated that sublethal stress induces MOMP in a small subpopulation of mitochondria within one cell (Figure 5). Furthermore, caspase activation occurring upon MOMP in a minor population of mitochondria was shown to be insufficient to induce cell death, but instead, it

drove DNA damage and genomic instability, which in turn triggered transformation and tumorigenesis (92).

4.5. Translation of Proteins

Mitochondria contain their own DNA and their own protein synthesis machinery, which enable the production of key subunits of the (DEFINE) oxidative phosphorylation (OXPHOS) machinery within mitochondria (93). Another important measure of mitochondrial functionality is therefore the assessment of mitochondrial protein translation. Classically, isolated mitochondria are incubated in the presence of radiolabeled methionine to assay the production of the few mitochondrially encoded proteins (94). However, recent advances have enabled the detection of mitochondrial translation in situ by utilizing the click chemistry–based fluorescent noncanonical amino acid-tagging (FUNCAT) procedure (95). During this assay, cells are cultured in the presence of the methionine analogs homopropargylglycine or azidohomoalanine, which get incorporated into nascent protein chains and are amenable to labeling with fluorophores by click chemistry. Because the mitochondrial ribosome is of bacterial origin, it is resistant to mammalian ribosome inhibitors, allowing the simultaneous block of cytosolic protein synthesis and effective labeling of mitochondrial protein synthesis in situ (96, 97). This revealed not only the localization of protein synthesis clusters within mitochondria (97) but also striking differences between individual organelles, especially within neuronal processes (96). Mitochondrial translation products were visualized all along the axon and within synaptic compartments (96), which has interesting implications for the assembly of the respiratory chain: As most OXPHOS complexes are a mosaic of nuclear and mitochondrial gene products, newly synthesized mitochondrial components must be matched by an influx of nuclear-encoded subunits (98). This strongly suggests that the biogenesis of mitochondria is not exclusive to the cell body but may happen all along the axon (reviewed in 99). How and where nuclear-encoded mitochondrial proteins are translated along the axon are areas of active research (100, 101) that greatly benefit from single-organelle analysis of mitochondrial functions.

SUMMARY POINTS

1. Advances and refinement of flow cytometers or spectral analyzers enable the multiparametric detection of nanometer-scale vesicles or particles to measure organelles

on a single-particle level.

2. The generation of fusion proteins of fluorescent markers with organelle-targeting sequences allows for microscopic live-cell imaging of organelles of interest.
3. Specific small-molecule dyes proved useful for the measurement of organelle properties, e.g., cationic dyes that accumulate in negatively charged mitochondrial matrix for the measurement of mitochondrial membrane potential.
4. Single-organelle analysis has revealed cell type–specific and location-specific adaptations within mitochondria that would have been overlooked in bulk analysis.

DISCLOSURE STATEMENT

The authors are not aware of any affiliations, memberships, funding, or financial holdings that might be perceived as affecting the objectivity of this review.

ACKNOWLEDGMENTS

This work was supported by the German Research Foundation to D.W. (WO 2158/1-1 and TRR179/TP13-Projektnummer 272983813) and (HA 7728/2-1 and EXC2145-A4/-B1) as well as the Max Planck Society (MPRGL) to A.B.G.. **[**AU: Spell out.**]**

LITERATURE CITED

1. Lang BF, Gray MW, Burger G. 1999. Mitochondrial genome evolution and the origin of eukaryotes. Annu. Rev. Genet. 33:351–97
2. West AP, Shadel GS, Ghosh S. 2011. Mitochondria in innate immune responses. Nat. Rev. Immunol. 11:389–402
3. Wanderoy S, Hees JT, Klesse R, Edlich F, Harbauer AB. 2020. Kill one or kill the many: interplay between mitophagy and apoptosis. Biol. Chem. 402:73–88
4. Attwell D, Laughlin SB. 2001. An energy budget for signaling in the grey matter of the brain. J. Cereb. Blood Flow Metab. 21:1133–45
5. Belanger M, Allaman I, Magistretti PJ. 2011. Brain energy metabolism: focus on astrocyte-neuron metabolic cooperation. Cell Metab. 14:724–38
6. Overly CC, Rieff HI, Hollenbeck PJ. 1996. Organelle motility and metabolism in axons versus

dendrites of cultured hippocampal neurons. J. Cell Sci. 109 (Part 5):971–80
7. Stauch KL, Purnell PR, Fox HS. 2014. Quantitative proteomics of synaptic and nonsynaptic mitochondria: insights for synaptic mitochondrial vulnerability. J. Proteome Res. 13:2620–36
8. Lewis TL, Jr., Kwon SK, Lee A, Shaw R, Polleux F. 2018. MFF-dependent mitochondrial fission regulates presynaptic release and axon branching by limiting axonal mitochondria size. Nat. Commun. 9:5008
9. Divakaruni SS, Van Dyke AM, Chandra R, LeGates TA, Contreras M, et al. 2018. Long-term potentiation requires a rapid burst of dendritic mitochondrial fission during induction. Neuron 100:860–75 e7
10. Wiesner RJ, Ruegg JC, Morano I. 1992. Counting target molecules by exponential polymerase chain reaction: copy number of mitochondrial DNA in rat tissues. Biochem. Biophys. Res. Commun. 183:553–59
11. Mansouri A, Gattolliat CH, Asselah T. 2018. Mitochondrial dysfunction and signaling in chronic liver diseases. Gastroenterology 155:629–47
12. Jost PJ, Grabow S, Gray D, McKenzie MD, Nachbur U, et al. 2009. XIAP discriminates between type I and type II FAS-induced apoptosis. Nature 460:1035–39
13. Ernster L, Schatz G. 1981. Mitochondria: a historical review. J. Cell Biol. 91:227s-55s
14. Faitg J, Davey T, Turnbull DM, White K, Vincent AE. 2020. Mitochondrial morphology and function: two for the price of one! J. Microsc. 278:89–106
15. Quintana A, Schwindling C, Wenning AS, Becherer U, Rettig J, et al. 2007. T cell activation requires mitochondrial translocation to the immunological synapse. PNAS 104:14418–23
16. Cieri D, Vicario M, Giacomello M, Vallese F, Filadi R, et al. 2018. SPLICS: a split green fluorescent protein-based contact site sensor for narrow and wide heterotypic organelle juxtaposition. Cell Death Differ. 25:1131–45
17. Cottet-Rousselle C, Ronot X, Leverve X, Mayol JF. 2011. Cytometric assessment of mitochondria using fluorescent probes. Cytometry A 79:405–25
18. Zhang S, Zhu S, Yang L, Zheng Y, Gao M, et al. 2012. High-throughput multiparameter analysis of individual mitochondria. Anal. Chem. 84:6421–28
19. Schneider A, Kurz S, Manske K, Janas M, Heikenwalder M, et al. 2019. Single organelle analysis to characterize mitochondrial function and crosstalk during viral infection. Sci. Rep. 9:8492

20. Ma L, Zhu S, Tian Y, Zhang W, Wang S, et al. 2016. Label-free analysis of single viruses with a resolution comparable to that of electron microscopy and the throughput of flow cytometry. Angew. Chem. Int. Ed. 55:10239–43
21. Rajotte D, Stearns CD, Kabcenell AK. 2003. Isolation of mast cell secretory lysosomes using flow cytometry. Cytometry A 55:94–101
22. Degtyarev M, Reichelt M, Lin K. 2014. Novel quantitative autophagy analysis by organelle flow cytometry after cell sonication. PLOS ONE 9:e87707
23. Fialka I, Steinlein P, Ahorn H, Bock G, Burbelo PD, et al. 1999. Identification of syntenin as a protein of the apical early endocytic compartment in Madin-Darby canine kidney cells. J. Biol. Chem. 274:26233–39
24. MacDonald JA, Bothun AM, Annis SN, Sheehan H, Ray S, et al. 2019. A nanoscale, multi-parametric flow cytometry-based platform to study mitochondrial heterogeneity and mitochondrial DNA dynamics. Commun. Biol. 2:258
25. Fecher C, Trovo L, Muller SA, Snaidero N, Wettmarshausen J, et al. 2019. Cell-type-specific profiling of brain mitochondria reveals functional and molecular diversity. Nat. Neurosci. 22:1731–42
26. Wyant GA, Abu-Remaileh M, Frenkel EM, Laqtom NN, Dharamdasani V, et al. 2018. NUFIP1 is a ribosome receptor for starvation-induced ribophagy. Science 360:751–58
27. Chen WW, Freinkman E, Wang T, Birsoy K, Sabatini DM. 2016. Absolute quantification of matrix metabolites reveals the dynamics of mitochondrial metabolism. Cell 166:1324–37.e11
28. Abu-Remaileh M, Wyant GA, Kim C, Laqtom NN, Abbasi M, et al. 2017. Lysosomal metabolomics reveals V-ATPase- and mTOR-dependent regulation of amino acid efflux from lysosomes. Science 358:807–13
29. Pflugradt R, Schmidt U, Landenberger B, Sanger T, Lutz-Bonengel S. 2011. A novel and effective separation method for single mitochondria analysis. Mitochondrion 11:308–14
30. Morris J, Na YJ, Zhu H, Lee JH, Giang H, et al. 2017. Pervasive within-mitochondrion single-nucleotide variant heteroplasmy as revealed by single-mitochondrion sequencing. Cell Rep. 21:2706–13
31. Presley AD, Fuller KM, Arriaga EA. 2003. MitoTracker Green labeling of mitochondrial proteins and their subsequent analysis by capillary electrophoresis with laser-induced fluorescence detection. J. Chromatogr. B Analyt. Technol. Biomed. Life Sci. 793:141–50

32. Friedman JR, Nunnari J. 2014. Mitochondrial form and function. Nature 505:335–43
33. Liesa M, Shirihai OS. 2013. Mitochondrial dynamics in the regulation of nutrient utilization and energy expenditure. Cell Metab. 17:491–506
34. Szabadkai G, Simoni AM, Chami M, Wieckowski MR, Youle RJ, Rizzuto R. 2004. Drp-1-dependent division of the mitochondrial network blocks intraorganellar Ca2+ waves and protects against Ca2+-mediated apoptosis. Mol. Cell 16:59–68
35. Suzuki R, Hotta K, Oka K. 2018. Transitional correlation between inner-membrane potential and ATP levels of neuronal mitochondria. Sci. Rep. 8:2993
36. Wolf DM, Segawa M, Kondadi AK, Anand R, Bailey ST, et al. 2019. Individual cristae within the same mitochondrion display different membrane potentials and are functionally independent. EMBO J. 38:e101056
37. Sivandzade F, Bhalerao A, Cucullo L. 2019. Analysis of the mitochondrial membrane potential using the cationic JC-1 dye as a sensitive fluorescent probe. Bio Protoc. 9:e3128
38. Perry SW, Norman JP, Barbieri J, Brown EB, Gelbard HA. 2011. Mitochondrial membrane potential probes and the proton gradient: a practical usage guide. BioTechniques 50:98–115
39. Jung DW, Davis MH, Brierley GP. 1989. Estimation of matrix pH in isolated heart mitochondria using a fluorescent probe. Anal. Biochem. 178:348–54
40. Bencina M. 2013. Illumination of the spatial order of intracellular pH by genetically encoded pH-sensitive sensors. Sensors 13:16736–58
41. Miesenbock G, De Angelis DA, Rothman JE. 1998. Visualizing secretion and synaptic transmission with pH-sensitive green fluorescent proteins. Nature 394:192–95
42. Orij R, Postmus J, Ter Beek A, Brul S, Smits GJ. 2009. In vivo measurement of cytosolic and mitochondrial pH using a pH-sensitive GFP derivative in Saccharomyces cerevisiae reveals a relation between intracellular pH and growth. Microbiology 155:268–78
43. Jankowski A, Kim JH, Collins RF, Daneman R, Walton P, Grinstein S. 2001. In situ measurements of the pH of mammalian peroxisomes using the fluorescent protein pHluorin. J. Biol. Chem. 276:48748–53
44. Reifenrath M, Boles E. 2018. A superfolder variant of pH-sensitive pHluorin for in vivo pH measurements in the endoplasmic reticulum. Sci. Rep. 8:11985
45. Santo-Domingo J, Giacomello M, Poburko D, Scorrano L, Demaurex N. 2013. OPA1 promotes pH flashes that spread between contiguous mitochondria without matrix protein

exchange. EMBO J. 32:1927–40
46. Picard M, Sandi C. 2021. The social nature of mitochondria: implications for human health. Neurosci. Biobehav. Rev. 120:595–610
47. Katayama H, Kogure T, Mizushima N, Yoshimori T, Miyawaki A. 2011. A sensitive and quantitative technique for detecting autophagic events based on lysosomal delivery. Chem. Biol. 18:1042–52
48. Pankiv S, Clausen TH, Lamark T, Brech A, Bruun JA, et al. 2007. p62/SQSTM1 binds directly to Atg8/LC3 to facilitate degradation of ubiquitinated protein aggregates by autophagy. J. Biol. Chem. 282:24131–45
49. Castillo K, Valenzuela V, Matus S, Nassif M, Onate M, et al. 2013. Measurement of autophagy flux in the nervous system in vivo. Cell Death. Dis. 4:e917
50. An H, Ordureau A, Korner M, Paulo JA, Harper JW. 2020. Systematic quantitative analysis of ribosome inventory during nutrient stress. Nature 583:303–9
51. Yoshii SR, Mizushima N. 2017. Monitoring and measuring autophagy. Int. J. Mol. Sci. 18:1865
52. Sun N, Yun J, Liu J, Malide D, Liu C, et al. 2015. Measuring in vivo mitophagy. Mol. Cell 60:685–96
53. McWilliams TG, Prescott AR, Allen GF, Tamjar J, Munson MJ, et al. 2016. mito-QC illuminates mitophagy and mitochondrial architecture in vivo. J. Cell Biol. 214:333–45
54. McWilliams TG, Prescott AR, Montava-Garriga L, Ball G, Singh F, et al. 2018. Basal mitophagy occurs independently of PINK1 in mouse tissues of high metabolic demand. Cell Metab. 27:439–49.e5
55. Pickrell AM, Youle RJ. 2015. The roles of PINK1, parkin, and mitochondrial fidelity in Parkinson's disease. Neuron 85:257–73
56. Valente EM, Abou-Sleiman PM, Caputo V, Muqit MM, Harvey K, et al. 2004. Hereditary early-onset Parkinson's disease caused by mutations in PINK1. Science 304:1158–60
57. Paul S, Pickrell AM. 2021. Hidden phenotypes of PINK1/Parkin knockout mice. Biochim. Biophys. Acta Gen. Subj. 1865:129871
58. Cornelissen T, Vilain S, Vints K, Gounko N, Verstreken P, Vandenberghe W. 2018. Deficiency of parkin and PINK1 impairs age-dependent mitophagy in Drosophila. eLife 7:e35878

59. Deshwal S, Fiedler KU, Langer T. 2020. Mitochondrial proteases: multifaceted regulators of mitochondrial plasticity. Annu. Rev. Biochem. 89:501–28
60. Sugiura A, McLelland GL, Fon EA, McBride HM. 2014. A new pathway for mitochondrial quality control: mitochondrial-derived vesicles. EMBO J. 33:2142–56
61. Ferree AW, Trudeau K, Zik E, Benador IY, Twig G, et al. 2013. MitoTimer probe reveals the impact of autophagy, fusion, and motility on subcellular distribution of young and old mitochondrial protein and on relative mitochondrial protein age. Autophagy 9:1887–96
62. Li H, Doric Z, Berthet A, Jorgens DM, Nguyen MK, et al. 2021. Longitudinal tracking of neuronal mitochondria delineates PINK1/Parkin-dependent mechanisms of mitochondrial recycling and degradation. Sci. Adv. 7:eabf6580
63. Bomba-Warczak E, Edassery SL, Hark TJ, Savas JN. 2021. Long-lived mitochondrial cristae proteins in mouse heart and brain. J. Cell Biol. 220:e202005193
64. Berridge MJ, Lipp P, Bootman MD. 2000. The versatility and universality of calcium signalling. Nat. Rev. Mol. Cell Biol. 1:11–21
65. McCormack JG, Halestrap AP, Denton RM. 1990. Role of calcium ions in regulation of mammalian intramitochondrial metabolism. Physiol. Rev. 70:391–425
66. Schild L, Keilhoff G, Augustin W, Reiser G, Striggow F. 2001. Distinct Ca2+ thresholds determine cytochrome c release or permeability transition pore opening in brain mitochondria. FASEB J. 15:565–67
67. Lampl S, Janas MK, Donakonda S, Brugger M, Lohr K, et al. 2020. Reduced mitochondrial resilience enables non-canonical induction of apoptosis after TNF receptor signaling in virus-infected hepatocytes. J. Hepatol. 73:1347–59
68. Davidson SM, Duchen MR. 2018. Imaging mitochondrial calcium fluxes with fluorescent probes and single- or two-photon confocal microscopy. Methods Mol. Biol. 1782:171–86
69. Grienberger C, Konnerth A. 2012. Imaging calcium in neurons. Neuron 73:862–85
70. Suzuki J, Kanemaru K, Iino M. 2016. Genetically encoded fluorescent indicators for organellar calcium imaging. Biophys. J. 111:1119–31
71. Kwon SK, Sando R 3rd, Lewis TL, Hirabayashi Y, Maximov A, Polleux F. 2016. LKB1 regulates mitochondria-dependent presynaptic calcium clearance and neurotransmitter release properties at excitatory synapses along cortical axons. PLOS Biol. 14:e1002516
72. Vaccaro V, Devine MJ, Higgs NF, Kittler JT. 2017. Miro1-dependent mitochondrial

positioning drives the rescaling of presynaptic Ca2+ signals during homeostatic plasticity. EMBO Rep. 18:231–40
73. De Vos KJ, Morotz GM, Stoica R, Tudor EL, Lau KF, et al. 2012. VAPB interacts with the mitochondrial protein PTPIP51 to regulate calcium homeostasis. Hum. Mol. Genet. 21:1299–311
74. Suzuki J, Kanemaru K, Ishii K, Ohkura M, Okubo Y, Iino M. 2014. Imaging intraorganellar Ca2+ at subcellular resolution using CEPIA. Nat. Commun. 5:4153
75. Suzanne M, Steller H. 2013. Shaping organisms with apoptosis. Cell Death Differ. 20:669–75
76. Nguyen TTM, Gillet G, Popgeorgiev N. 2021. Caspases in the developing central nervous system: apoptosis and beyond. Front. Cell Dev. Biol. 9:702404
77. Labi V, Erlacher M. 2015. How cell death shapes cancer. Cell Death. Dis. 6:e1675
78. Barber GN. 2001. Host defense, viruses and apoptosis. Cell Death Differ. 8:113–26
79. Strasser A, Harris AW, Huang DC, Krammer PH, Cory S. 1995. Bcl-2 and Fas/APO-1 regulate distinct pathways to lymphocyte apoptosis. EMBO J. 14:6136–47
80. Pihan P, Carreras-Sureda A, Hetz C. 2017. BCL-2 family: integrating stress responses at the ER to control cell demise. Cell Death Differ. 24:1478–87
81. Susnow N, Zeng L, Margineantu D, Hockenbery DM. 2009. Bcl-2 family proteins as regulators of oxidative stress. Semin. Cancer Biol. 19:42–49
82. Tait SW, Green DR. 2010. Mitochondria and cell death: outer membrane permeabilization and beyond. Nat. Rev. Mol. Cell Biol. 11:621–32
83. Hao Z, Mak TW. 2010. Type I and type II pathways of Fas-mediated apoptosis are differentially controlled by XIAP. J. Mol. Cell Biol. 2:63–64
84. Lartigue L, Kushnareva Y, Seong Y, Lin H, Faustin B, Newmeyer DD. 2009. Caspase-independent mitochondrial cell death results from loss of respiration, not cytotoxic protein release. Mol. Biol. Cell 20:4871–84
85. Tait SW, Ichim G, Green DR. 2014. Die another way—non-apoptotic mechanisms of cell death. J. Cell Sci. 127:2135–44
86. Tait SW, Green DR. 2008. Caspase-independent cell death: leaving the set without the final cut. Oncogene 27:6452–61
87. Goldstein JC, Waterhouse NJ, Juin P, Evan GI, Green DR. 2000. The coordinate release of

cytochrome c during apoptosis is rapid, complete and kinetically invariant. Nat. Cell Biol. 2:156–62

88. Deshmukh M, Kuida K, Johnson EM, Jr. 2000. Caspase inhibition extends the commitment to neuronal death beyond cytochrome c release to the point of mitochondrial depolarization. J. Cell Biol. 150:131–43
89. Martinou I, Desagher S, Eskes R, Antonsson B, Andre E, et al. 1999. The release of cytochrome c from mitochondria during apoptosis of NGF-deprived sympathetic neurons is a reversible event. J. Cell Biol. 144:883–89
90. Colell A, Ricci JE, Tait S, Milasta S, Maurer U, et al. 2007. GAPDH and autophagy preserve survival after apoptotic cytochrome c release in the absence of caspase activation. Cell 129:983–97
91. Tait SW, Parsons MJ, Llambi F, Bouchier-Hayes L, Connell S, et al. 2010. Resistance to caspase-independent cell death requires persistence of intact mitochondria. Dev. Cell 18:802–13
92. Ichim G, Lopez J, Ahmed SU, Muthalagu N, Giampazolias E, et al. 2015. Limited mitochondrial permeabilization causes DNA damage and genomic instability in the absence of cell death. Mol. Cell 57:860–72
93. Mai N, Chrzanowska-Lightowlers ZM, Lightowlers RN. 2017. The process of mammalian mitochondrial protein synthesis. Cell Tissue Res. 367:5–20
94. Chomyn A. 1996. In vivo labeling and analysis of human mitochondrial translation products. Methods Enzymol. 264:197–211
95. Dieterich DC, Hodas JJ, Gouzer G, Shadrin IY, Ngo JT, et al. 2010. In situ visualization and dynamics of newly synthesized proteins in rat hippocampal neurons. Nat Neurosci 13:897–905
96. Yousefi R, Fornasiero EF, Cyganek L, Montoya J, Jakobs S, et al. 2021. Monitoring mitochondrial translation in living cells. EMBO Rep. 22:e51635
97. Zorkau M, Albus CA, Berlinguer-Palmini R, Chrzanowska-Lightowlers ZMA, Lightowlers RN. 2021. High-resolution imaging reveals compartmentalization of mitochondrial protein synthesis in cultured human cells. PNAS 118:e2008778118
98. Richter-Dennerlein R, Oeljeklaus S, Lorenzi I, Ronsor C, Bareth B, et al. 2016. Mitochondrial protein synthesis adapts to influx of nuclear-encoded protein. Cell 167:471–

83.e10

99. Harbauer AB. 2017. Mitochondrial health maintenance in axons. Biochem. Soc. Trans. 45:1045–52

100. Cioni JM, Lin JQ, Holtermann AV, Koppers M, Jakobs MAH, et al. 2019. Late endosomes act as mrna translation platforms and sustain mitochondria in axons. Cell 176:56–72.e15

101. Kuzniewska B, Cysewski D, Wasilewski M, Sakowska P, Milek J, et al. 2020. Mitochondrial protein biogenesis in the synapse is supported by local translation. EMBO Rep. 21:e48882

TERMS AND DEFINITION LIST:

Mitochondrial membrane potential: generated by proton pumps across the inner mitochondrial membrane and the driving force for ATP generation

Mitophagy: the specific elimination of damaged mitochondria via autophagy preventing the presence of dysfunctional mitochondria

Heteroplasmy: the presence of more than one mitochondrial DNA (mtDNA) variant within an individual cell

Oxidative phosphorylation: a metabolic process within mitochondria, where electron transfer to oxygen is coupled to production of ATP

FAMS: fluorescent-activated mitochondrial sorting separates mitochondrial subpopulations according to size, ultrastructure, MMP, and mtDNA copy number in special setups of FACS

Mitochondrial outer membrane permeabilization: triggered by oligomerization of Bax/Bak at the mitochondrial outer membrane preceding the release of cytochrome c

Förster resonance energy transfer (FRET): transfer of excitation energy from one molecule to another depending on their close association